PHYSICAL REVIEW A VOLUME 41, NUMBER 9 1 MAY 1990

Laser effects in photoionization. II. Numerical solution of coupled equations for atomic hydrogen

K. J. LaGattuta
Applied Theoretical Physics Division, Los Alamos National Laboratory, Los Alamos, New Mexico 87545

(Received 1 December 1989)

The time-dependent Schrödinger equation was solved numerically, as a set of coupled equations, for an electron moving in three spatial dimensions, bound initially in the ground state of a hydrogen atom, and acted upon by a linearly polarized, single-frequency, classical electromagnetic field, turned on abruptly at $t=0$. Characteristic photoionization times $\tau_{\rm PI}$ were computed for a wide range of laser intensities, at a photon energy of 5 eV. Comparison was made with the predictions of two widely used analytic expressions for $\tau_{\rm PI}$. Emitted electron energy spectra and angular distributions were computed. The spectrum of radiation emitted during ionization was also determined.

I. INTRODUCTION

The application of direct numerical methods to the calculation of multiphoton photoionization rates, and characteristic photoionization times, for atomic systems, has just recently become technically feasible. Prior semianalytic work[1] on the photoionization of atomic hydrogen has now been supplanted by these direct solutions of the time-dependent Schrödinger equation for hydrogenic systems.[2,3] Calculation of photoionization times for multielectron atoms and ions has also begun, although those time-dependent Hartree-Fock based approaches are essentially still one electron in nature.[4]

In this paper we report results of the application of a code describing the interaction of a linearly polarized, single frequency, laser beam with hydrogenic ions,[3] to the calculation of multiphoton photoionization times $\tau_{\rm PI}$, emitted electron energy spectra and angular distributions, for atomic hydrogen. A wide range of laser intensities was considered, at the single laser photon energy of 5 eV. The spectrum of radiation emitted during ionization was also determined.

The intent of this work was to compare in detail the outcome of these rather precise calculations with the widely used analytic, but approximate, formulas of (a) Reiss,[5] for multiphoton absorption (when the photon energy is not "too low"; (b) Keldysh,[6] in the so-called tunneling limit (when the photon energy is "very low"). A similar study has already been performed for the case of an electron moving in one spatial dimension (1D) and bound initially by a δ potential.[7] We also expected to be able to compare our results with the recent experiments performed by Kyrala on multiphoton ionization of atomic hydrogen.[8]

II. NUMERICAL METHODS

The numerical method has been described in an earlier publication.[3] We recapitulate here the essential features of this approach.

We write the time-dependent Schrödinger equation for this problem as

$$\left[-\tfrac{1}{2}\nabla^2-\frac{1}{r}+\mathbf{r}\cdot\mathbf{E}(t)-\frac{id}{dt}\right]\psi(\mathbf{r},t)=0\ , \qquad (1)$$

where the driving (linearly polarized laser electric) field is represented by

$$\mathbf{E}(t)=-\hat{\mathbf{z}}E_0\cos(w_0t+\phi_0)\theta(t)\ . \qquad (2)$$

ϕ_0 is the phase of the electric field at the moment of laser turn-on, $\theta(t)$ is the unit step function, and all quantities are in atomic units (a.u.). For $t\leq 0$, the wave function is given by $\psi(\mathbf{r},t)=\phi_{1s}(r)Y_{00}(\hat{\mathbf{r}})\exp(-\varepsilon_{1s}t)$, where $\varepsilon_{1s}=-0.5$. Throughout these calculations, the phase was chosen to be either $\phi_0=0$ or $\phi_0=\pi$.

For $t>0$, we first expand $\psi(\mathbf{r},t)$ in spherical harmonics. Thus components of the time-dependent wave function, labeled by orbital angular momentum quantum number l are coupled, via interaction with the driving field, to components labeled by $l\pm1$. Since the axis of quantization is taken to lie along the applied electric field [see Eq. (2)], the azimuthal quantum number m is conserved. Second, the radial coordinate r is discretized; the mesh-size Δr is taken to be independent of r.

The full time-dependent Schrödinger equation then appears as a set of coupled finite difference equations, which are first order in t; see Eq. (7) of Ref. 3. This set of equations is solved numerically, in the time domain, by means of a standard predictor-corrector scheme. Next, the computed wave function $\psi(\mathbf{r},t)$ is projected onto the 1s state of hydrogen, $\phi_{1s}(r)=2\exp(-r)$, in order to determine the probability $P_{1s}(t)$ of remaining bound in 1s, at any time $t>0$; i.e.,

$$P_{1s}(t)=\left|\int d\mathbf{r}\,\psi^*(\mathbf{r},t)\phi_{1s}(r)Y_{00}(\hat{\mathbf{r}})\right|^2\ , \qquad (3)$$

where $P_{1s}(0)=1$, since $\psi(\mathbf{r},0)=\phi_{1s}\ (r)Y_{00}(\hat{\mathbf{r}})$. Finally, the curve of $P_{1s}(t)$ vs t is fit to a single exponential of the form $\exp(-t/\tau_{\rm PI})$, and the characteristic photoionization time $\tau_{\rm PI}$ thereby determined. Note that, as in our previous work,[3,7] the driving field is turned on abruptly at $t=0$ [see Eq. (2)].

Parts of this calculation required special care: (a) It was necessary to ensure that no significant amount of probability density was generated beyond the maximum included value of the radial coordinate $r_{\max}$; i.e.,

$$\int d\hat{\mathbf{r}} \int_0^{r_{\max}} dr\, r^2 |\psi(\mathbf{r},t)|^2 \approx 1 \tag{4}$$

for all $0 \leq t \leq t_{\max}$, where $t_{\max}$ was the maximum value of the time. Absorbing potentials were not employed in these calculations. (b) It was important to be sure that $t_{\max}$ was large enough for true ionization to have occurred; e.g., in some cases, Rabi oscillations in ground-state population obscured the ionization event. (c) It was necessary to demonstrate the convergence of computed quantities in both l and Δr; e.g., the range of l values had to be large enough, and the value of Δr small enough, to produce an accurate $\tau_{\rm PI}$. As described in Ref. 3, since convergence in Δr was quite slow, it was usually necessary to extrapolate results to $\Delta r = 0$.

The abrupt turn on of the laser electric field [see Eq. (2)] introduces an essential, but easily isolatable small transient, into the early time values of the probability density. Also, a certain amount of high-frequency noise is thereby introduced into the corresponding emitted electron kinetic energy spectra, and into the emitted radiation spectra. However, for the laser parameters considered here, this high-frequency noise occurs with a relatively low amplitude, and is readily distinguished from the main spectral features. We point out that, for weaker laser fields than those described here, the abrupt turn on can lead to the appearance of even harmonics of the laser frequency in the emitted radiation spectrum.

Finally, it must be recognized that the general form of the curve of $P_{1s}(t)$ vs t, is not a perfect single exponential. The fit of such a curve to a single exponential, although convenient for purposes of tabulation, is therefore very much subject to fitting errors; e.g., for a given curve of $P_{1s}(t)$ vs t, the range of t values included in the fit is often a critical determinant of the resulting $\tau_{\rm PI}$ value. Such considerations can easily lead to a 25% "uncertainty" in the computed $\tau_{\rm PI}$, even though the numerical solution of the Schrödinger equation may be converged to better than 1%, for all $r \leq_{\max}$ and $t \leq t_{\max}$. This effect is particularly troublesome at, or in the neighborhood of a resonance. Questions relating to gauge have been discussed in Ref. 7.

III. RESULTS

A. Photoionization time

Results obtained from calculations of characteristic photoionization times $\tau_{\rm PI}$, performed as outlined in the preceding section, appear in Fig. 1; values of $\tau_{\rm PI}$ vs laser intensity I_0 are plotted for the photon energy of $\omega_0 = 5$ eV. For comparison, values of $\tau_{\rm II}$ obtained by the method of Reiss [Eq. (5) of Ref. 5, with the correct hydrogenic 1s wave function], and as predicted by the tunneling formula of Keldysh [Eq. (1) of Ref. 6, in the small ω_0 limit], are included.

It is apparent that neither of the two approximate formulas are at all adequate for describing the variation of $\tau_{\rm PI}$ with I_0, for the photoionization of ground-state hydrogen by 5 eV photons. Typically, the discrepancy between either of the approximate formulas, and values of $\tau_{\rm PI}$ obtained from the detailed solution of Eq. (1), are a factor of 10, but can be as great as a factor of a hundred or more, especially at the lower laser intensities.

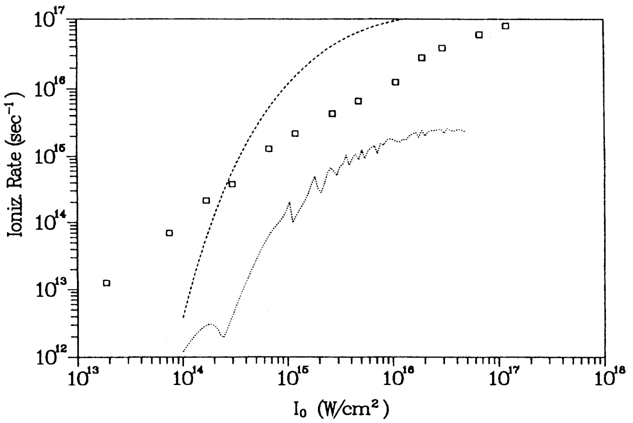

FIG. 1. Photoionization rate vs laser intensity for the 1s state of 3D hydrogen; $\omega_0 = 5$ eV. Our values (□); tunneling limit of Keldysh (— — —); Reiss (· · · ·).

This large discrepancy between values of $\tau_{\rm PI}$ obtained from the approximate formulas and from the detailed solution of the Schrödinger equation, for almost all values of I_0, was not observed in our previous study of the 1D δ potential.[7] In Fig. 2 we plot values of $\tau_{\rm PI}$ obtained from the solution of the Schrödinger equation for the 1D δ potential, along with the predictions of the analogous approximate formulas[7] (Reiss and Keldysh). The discrepancies, in this case, are typically less than an order of magnitude.

It has been widely conjectured that the dominant influences on the characteristic photoionization time of an initially bound electron are the laser intensity, laser photon energy, and electron binding energy, for fixed

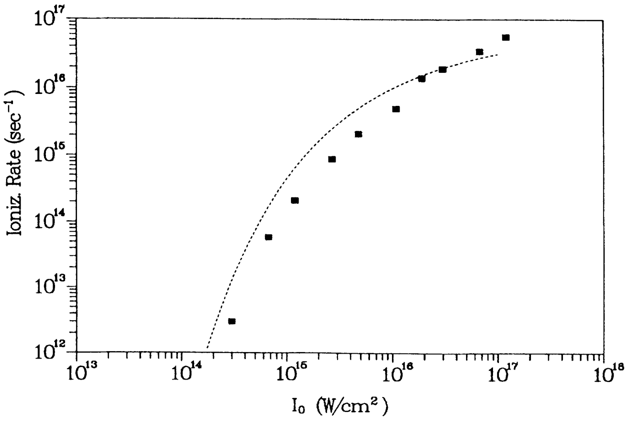

FIG. 2. Photoionization rate vs laser intensity, for the 1D δ potential, with binding energy $-$ 0.5 a.u. Our values (■); tunneling limit of Keldysh analog (— — —); Reiss analog (· · · ·).

laser polarization; i.e., for multiphoton processes. As a comment on this conjecture, we plot in Fig. 3 values of $\tau_{\rm PI}$ obtained by us, via the method described above and in Ref. 7, for both the ground state of 3D hydrogen, and for the 1D δ potential with binding energy − 0.5. a.u. (these are the same values that appeared in Figs. 1 and 2.)

From Fig. 3 one sees that the time required to photoionize a 1s electron from 3D hydrogen is considerably shorter than that required to photoionize an electron bound initially by 0.5 a.u., in a 1D δ potential; i.e., for 5 eV photons, over a range of laser intensities $10^{13} \leq I_0 \leq 10^{16}$ W/cm^2. Note that at the lower intensities the discrepancy is greater. We ascribe this difference to the influence of the two photon resonance, which strongly affects the photoionization process for 3D hydrogen, but not for the 1D δ potential, especially at the lower laser intensities. We refer here to the two-step resonance process described by

$$1s + 2\gamma \rightarrow 2s \ ,$$
$$2s + \gamma \rightarrow \text{continuum electron} \ . \qquad (5)$$

At $I_0 = 0$, a photon energy of $\omega_0 = 5.102$ eV would place the process of Eq. (5) into exact resonance. For $I_0 > 0$, the required photon energy would be somewhat higher.

We should point out that, for the high field strengths which are the subject of these calculations, the resonance discussed above will be quite broad. Moreover, substantial mixing of the 2s and 2p levels will occur during the ionization event. See the following subsections (B and C) for further discussion.

B. Electron kinetic energy spectra

The spectrum of emitted electron kinetic energies, for multiphoton photoionization of atomic hydrogen, has been measured[8] in recent experiments. These data were all taken with a linearly polarized laser electric field, for a photon energy of 5 eV, and over a range of laser intensities $10^{13} \leq I_0 \leq 10^{16}$ W/cm^2. Calculations of such emitted electron kinetic energy spectra, have heretofore been based almost entirely on the approximate expressions due to Reiss.[5]

We present here the first emitted electron kinetic energy spectra, for atomic hydrogen, to be obtained from direct solutions of the time-dependent Schrödinger equation [Eq. (1)] for this system. We define the differential probability of appearing in a continuum state of the Coulomb potential, labeled by $k = \sqrt{2E_k}$ and summed over continuum partial wave l_c, as

$$\frac{dP_k(t)}{dE_k} = \sum_{l_c} \left| \int d\mathbf{r}\,\psi^*(\mathbf{r},t)\Phi_{k,l_c}(r)Y_{l_c,0}(\hat{\mathbf{r}}) \right|^2 \qquad (6)$$

where $\psi(\mathbf{r},t)$ is the solution of Eq. (1), and Φ_{k,l_c} is the Coulomb continuum solution,[9,10] with no external field. The spectra determined in this fashion are time-dependent, oscillating with the frequency ω_0 of the driving laser electric field. The corresponding zero field spectra, accessible experimentally, are given by Eq. (6) at those times for which $\mathbf{E}(t)$ is a maximum.[7] The total probability of being in the continuum is $\int_0^\infty dE_k dP_k(t)/dE_k$.

In Fig. 4 we plot values of dP_k/dE_k vs E_k for a linearly polarized laser electric field, with $\omega_0 = 0.184$ a.u. (5 eV) and $I_0 = 2.42 \times 10^{14}$ W/cm^2, for an emitted electron which was bound initially in a 1s state of atomic hydrogen. The calculation was performed with ten partial waves ($0 \leq l \leq 9$), on a uniform radial grid with $\Delta r = 0.30$ a.u., and with $r_{\max} = 100$ a.u. The spectrum was sampled at $t = t_{\rm plot} = 7\pi/\omega_0 = 120$ a.u., a time for which P_{1s} has fallen to a value of ~ 0.38. The total probability in the continuum at this time is 0.46; the average value of the continuum energy is 0.073 a.u.

Several features which appear in Fig. 4 should be remarked: (1) Within the limitations imposed by the finite-size griding, the position of the lowest-energy peak in the spectrum is consistent with the predicted value[11]

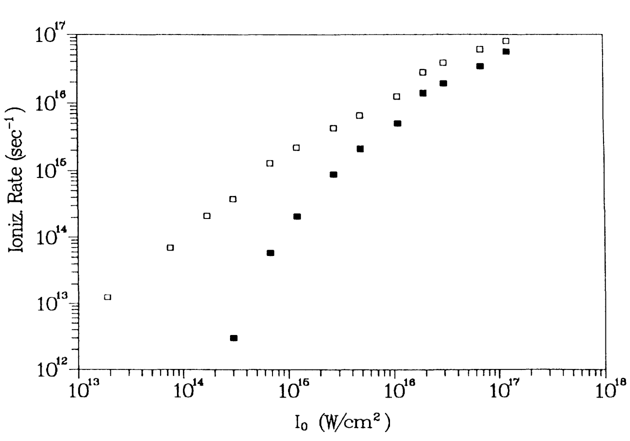

FIG. 3 Photoionization rate vs laser intensity for 1s state of 3D hydrogen (□); 1D δ potential with binding energy − 0.5 a.u. (■).

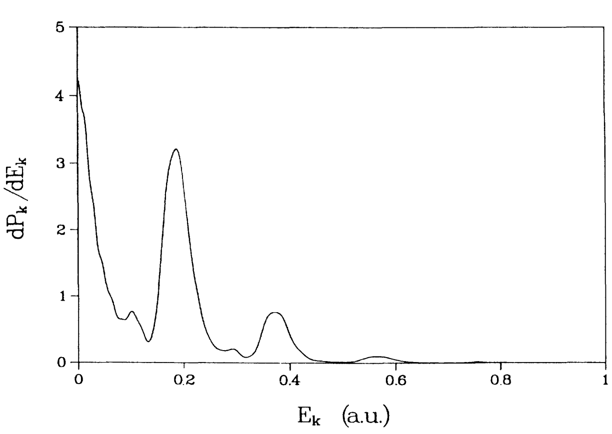

FIG. 4 Emitted electron kinetic energy spectrum, for the 1s state of 3D hydrogen, with $\omega_0 = 5$ eV and $I_0 = 2.42 \times 10^{14}$ W/cm^2, summed over all l_c.

i.e., $E_k = 3\omega_0 - 0.5 - I_0/(4\omega_0^2) \approx 0.001$ a.u., which includes the full ponderomotive shift. (2) ATI peaks are separated from the first (threshold) ionization peak by multiples of ω_0, and appear with decreasing amplitude. Essentially only three or four peaks are observed. This is consistent with the experiment.[8] (3) The width of the individual peaks is $\Delta E_k \approx 0.058$ a.u.

The characteristic photoionization time for this case is determined to be $\tau_{\mathrm{PI}} \approx 124$ a.u. so one might conjecture generally that the width $\Delta E_k \sim 2\pi/\tau_{\mathrm{PI}}$. This is, however, incorrect. Sampling of the spectrum at later times shows instead that $\Delta E_k \sim 2\pi/t_{\mathrm{plot}}$. That is, the value of ΔE_k is entirely a consequence of the sharp turnoff in the time record at t_{plot} (and the sharp turn on at $t=0$). We note that the value of τ_{PI} quoted here is for $\Delta r = 0.30$. Computations of τ_{PI} performed at larger values of Δr, and extrapolation to $\Delta r = 0$, gave finally $\tau_{\mathrm{PI}} \approx 160$ a.u.; see remarks following Eq. (4).

The occupation of the various continuum partial waves is also of some interest. In Figs. 5(a) and 5(b) we plot electron spectra for odd and even values of l_c, respectively. Conditions are as in Fig. 4, where the sum over all partial waves appeared. We note that the threshold ("three photon," at $E_k \approx 0.00$ a.u.) peak is dominated by $l_c = 1$, in accord with the notion that this is a near resonant process, as described by Eq. (5). However, a peak at $l_c = 3$ appears with almost equal probability, and this does not accord with the simple resonance hypothesis. Moreover, the first ATI peak ("four photon," at $E_k \approx 0.19$ a.u.) is dominated by odd partial waves, while the second ATI peak ("five photons," at $E_k \approx 0.37$ a.u.) is dominated by even partial waves. If the resonance hypothesis were strictly true, then the first ATI peak should contain only even partial waves and the second ATI peak only odd partial waves. It appears then that there is a substantial mixing of 2*s* and 2*p* states during the ionization event, and that ionization occurs from both the 2*s* and 2*p* states.

In support of the preceding view, we plot in Fig. 6 values of the probability to be in each of the $n=2$ levels, as well as in the ground state. It is clear from the figure that the 2*p* level is populated preferentially, and that ionization occurs primarily from that state. However, there is some transient occupation of the 2*s* level too, especially at early times, and threshold ionization evidently occurs largely from that state.

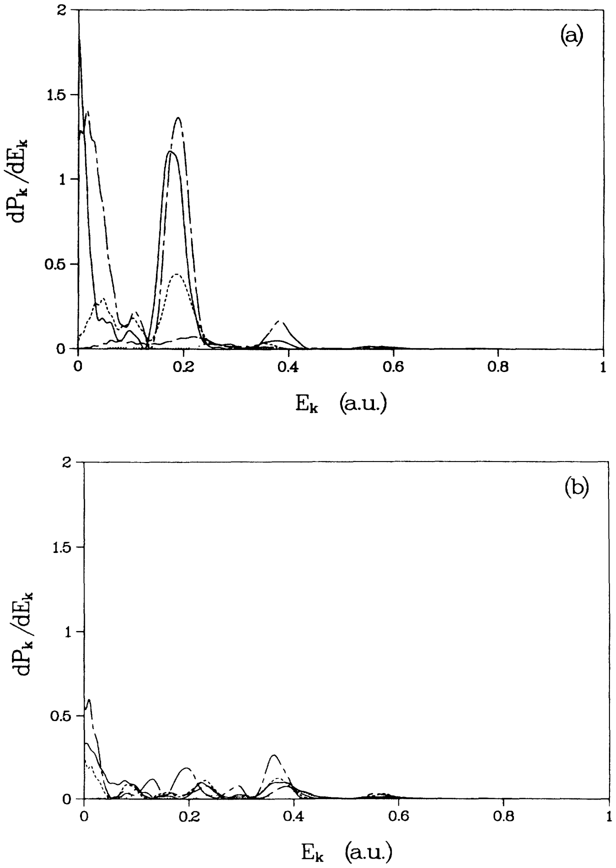

FIG. 5 Emitted electron energy spectrum by (a) (odd) partial wave; conditions as in Fig. 4: $l_c=1$ (——); $l_c=3$ (– – – -); $l_c=5$ (— — —); $l_c=7$ (—·—·—·); $l_c=9$ (· · · ·). (b) (even) partial wave; conditions as in Fig. 4: $l_c=0$ (——); $l_c=2$ (– – – -); $l_c=4$ (— — —); $l_c=6$ (—·—·—·); $l_c=8$ (· · · ·).

C. Electron angular distributions

There appears to be some consensus[12] that, at the intensities being discussed here, the emitted electron angular distributions which are measured experimentally do not usually reflect the details of the ionization event itself. Instead these measured quantities are determined largely by the shape of the laser focal volume, and are the result of varying amounts of pondermotive acceleration (deflection) imparted to the ionized electron as it leaves the interaction region. Considerations of laser temporal pulse shape also must generally play a role here.

Nevertheless, we include in this report the results of our calculations of emitted electron angular distributions, if for no other reason than to facilitate comparison with other (yet to appear) calculations. The results which we describe here are, to the best of our knowledge, the first such emitted electron angular distributions to have been

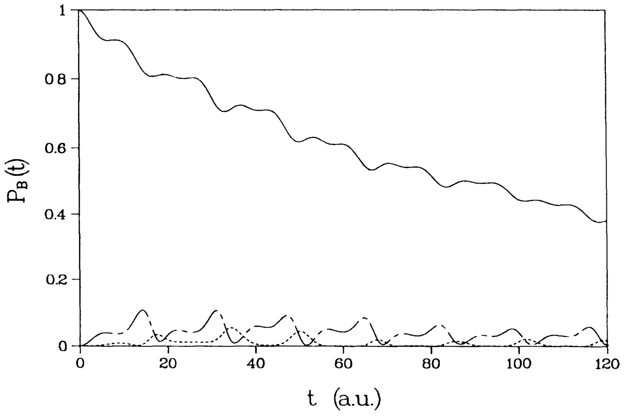

FIG. 6 Bound-state probabilities vs time conditions as in Fig. 4; $P_{1s}(t)$ (——); $P_{2p}(t)$ (– – – -); $P_{2s}(t)$ (— — —).

obtained by direct solution of the time-dependent Schrödinger equation, for 3D hydrogen.

In Fig. 7 we plot values of the doubly differential probability of appearing in a continuum state of the Coulomb potential, propagating at an angle θ relative to the z axis (direction of the laser electric field) and with a continuum energy E_k. This probability is defined as

$$\frac{dP_k^2(t;\theta)}{d\theta\, dE_k}=2\pi\left|\sum_{l_c} Y_{l_c,0}^*(\hat{\mathbf{k}})\int d\mathbf{r}\,\psi^*(\mathbf{r},t)\Phi_{k,l_c}(r)Y_{l_c,0}(\hat{\mathbf{r}})\right|^2 , \tag{7}$$

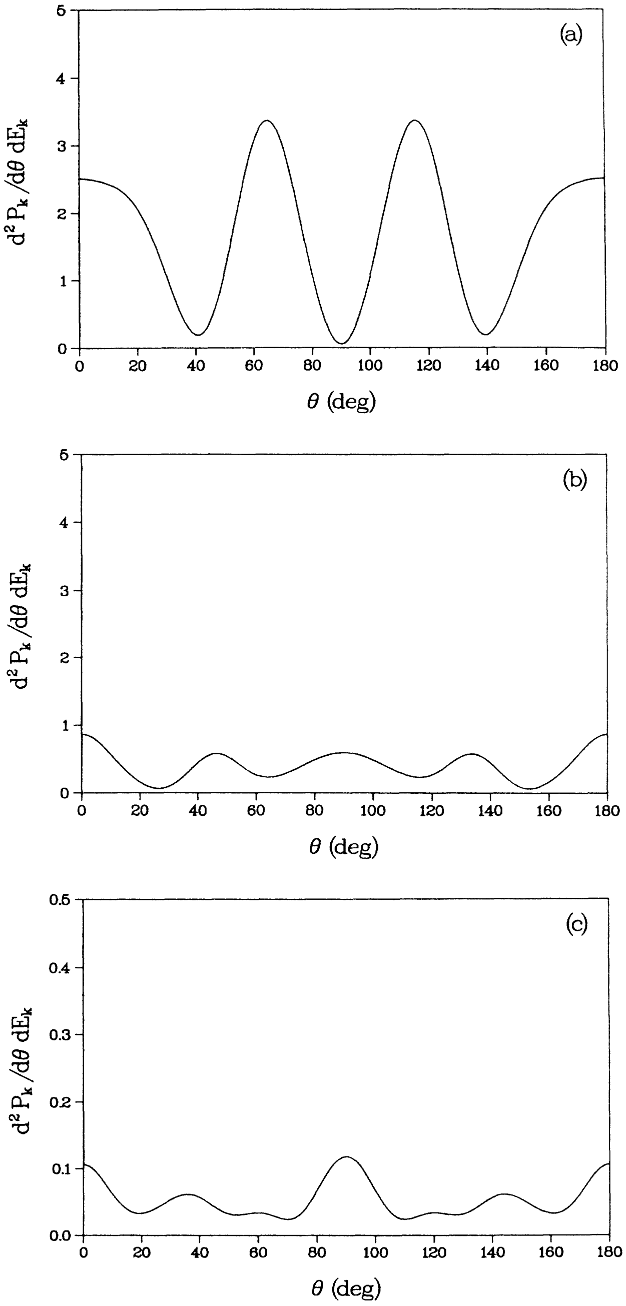

FIG. 7 Emitted electron angular distribution for (a) $E_k=0.19$ a.u.; (b) $E_k=0.37$ a.u.; (c) $E_k=0.56$ a.u.; conditions as in Fig. 4.

where Φ_{k,l_c} is the continuum Coulomb wave function,[9,10] labeled by $k=\sqrt{2E_k}$, and by the partial wave l_c. Conditions are as in Fig. 4. The plotted distribution, discussed below, has been symmetrized; i.e., results obtained with the starting phases $\phi_0=0$ and $\phi_0=\pi$ [Eq. (2)] have been averaged.

The angular dependence of $d^2P_k(t;\theta)/d\theta\, dE_k$ which appears in Fig. 7 is complex, generally exhibiting relatively large peaks at angles other than $\theta=0$ and $\theta=\pi$, for all values of the continuum energy E_k. Whereas, for an ionization process unaffected by atomic structure, one would only expect to see peaks along the z axis;[3,13] e.g., for a pure p wave continuum. The existence of peaks in $dP_k^2(t;\theta)/d\theta\, dE_k$ off the z axis is therefore evidence of the "resonance" nature of the ionization process, for this choice of laser parameters.[13] The structure appears to reflect the presence of both odd and even partial waves in the emitted electron energy spectrum; i.e., since the resonance intermediate state is a mixture of $l=0$ and $l=1$ partial waves. See the remarks appearing in the preceding subsections (A and B).

D. Spectrum of emitted radiation

The spectral density of (dipole) radiation emitted during the ionization event was determined according to[7]

$$S(\Omega)=\frac{\alpha^3}{3\pi}\left|\int dt\, e^{i\Omega t}\frac{d^2\langle z(t)\rangle}{dt^2}\right|^2 , \tag{8}$$

where $\int d\Omega\, S(\Omega)=(2\alpha^3/3)\int dt|d^2\langle z(t)\rangle/dt^2|^2$ is the total radiated energy, and $\langle z(t)\rangle\equiv\int d\mathbf{r}|\psi(\mathbf{r},t)|^2 z$. Note that, since this problem possesses azimuthal symmetry, then $\langle x(t)\rangle=\langle y(t)\rangle$, for all t.

For the conditions of Fig. 4, the spectrum of emitted radiation appears in Fig. 8. As expected, even harmonics of the fundamental laser frequency $\omega_0\approx0.184$ a.u. (5 eV) are absent. The third harmonic, at $\Omega\approx0.55$ a.u., is the strongest feature in the spectrum while the fifth harmonic is just barely visible.

We include, for purposes of comparison, in Figs. 9(a) and 9(b) plots of $S(\Omega)$ vs Ω for laser frequencies

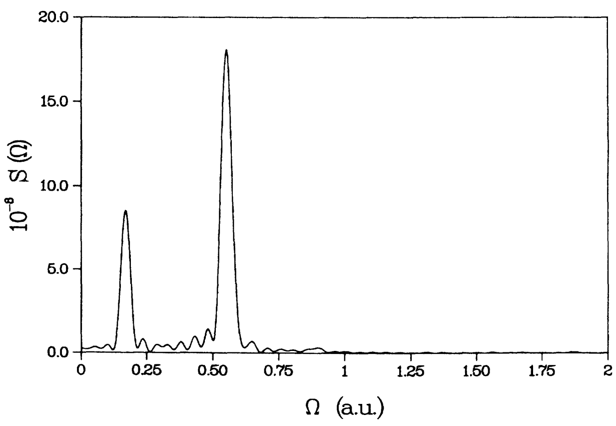

FIG. 8 Spectral density of emitted radiation; conditions as in Fig. 4.

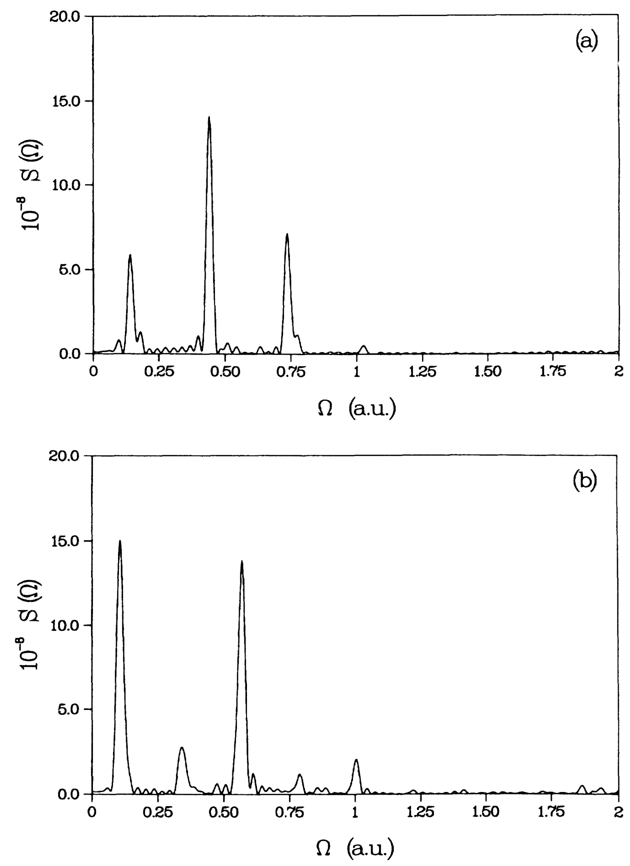

FIG. 9 (a) Spectral density of emitted radiation; conditions as in Fig. 4., except (a) $\omega_0=4$ eV. (b) $\omega_0=3$ eV.

$\omega_0 \approx 0.147$ a.u. (4 eV) and $\omega_0 \approx 0.110$ a.u. (3 eV), respectively; both at $I_0=2.42\times10^{14}$ W/cm^2. In Fig. 9(a) the third harmonic, at $\Omega\approx0.44$ a.u., is the most prominent feature, but the fifth harmonic is also quite intense; the seventh harmonic has essentially negligible intensity. In Fig. 9(b) the fifth harmonic, at $\Omega\approx0.55$ a.u., is very prominent, while higher harmonics are very weak.

These observations accord with the notion[14] that the maximum harmonic $n_{\max}$ radiated during ionization obeys the relationship $n_{\max}\,\omega_0\approx0.5$, where ω_0 is the fundamental laser frequency and $-$ 0.5 a.u. is the binding energy.

IV. DISCUSSION AND SUMMARY

The effects of atomic structure on the multiphoton ionization of atomic hydrogen, initially in its ground state, have been demonstrated for a laser photon energy of $\omega_0=5$ eV, and for laser intensities $I_0\lesssim10^{16}$ W/cm^2, through direct solution of the time-dependent Schrödinger equation [Eq. (1)]. These effects pertain to (a) the shortening of the characteristic photoionization time $\tau_{\rm PI}$ for ionization of 3D hydrogen, as compared to the 1D δ potential; (b) The existence of complex structures in the emitted electron energy spectra; (c) the existence of complex structures in the emitted electron angular distributions. All of these effects may be traced to the transient excitation of the $n=2$ levels (both $2s$ and $2p$), with subsequent ionization from these levels.

Indeed, the behavior of the photoionization rate, displayed in Fig. 1, directly reflects the presence of this resonance. That is, the photoionization rate is seen to vary approximately linearly with the laser intensity I_0 (over the range $10^{13}\lesssim I_0\lesssim10^{16}$ W/cm^2). One expects, on general principles,[15] that the rate for the process of Eq. (5) will follow the law

$$\frac{1}{\tau_{\rm PI}}\propto I_0^2\frac{\Gamma(I_0)}{\{[2\omega_0-\varepsilon_{2s}(I_0)]^2+\frac{1}{4}\Gamma^2(I_0)\}} \tag{9}$$

where $\Gamma(I_0)$ is the intensity dependent resonance width and $\varepsilon_{2s}(I_0)$ the resonance energy. For sufficiently large values of I_0, the width should be proportional to I_0, so that $1/\tau_{\rm PI}\propto I_0$.

The large discrepancies between the approximate formulas of Reiss and Keldysh, and the results of our numerical calculations, are not surprising in retrospect. After all, those formulas were not intended[5,6] to describe resonance phenomena. Unfortunately, one does not know *a priori* how close to a resonance one must be in order to render such formulas inapplicable nor what their accuracy is generally. In any case, we have shown here their inapplicability for a widely used wavelength (248 nm), or photon energy(5 eV), for experiments on atomic hydrogen. At intensities $I_0\gtrsim10^{16}$ W/cm^2, the effects of atomic structure become less important. See Fig. 3, where results for 3D hydrogen and the 1D δ potential are compared. As pointed out in an earlier paper,[3] in this region of intensities, the characteristic photoionization time can be well represented by the simple formula

$$\tau_{\rm PI}=(1/\omega_o)\sin^{-1}(\omega_0/\sqrt{I_0}) \tag{10}$$

in a.u., for the laser electric field of Eq. (2), with $\phi_0=0$, and when $\omega_0^2\leq I_0$. This is the so-called semiclassical region.[7]

The spectrum of radiation emitted during ionization has been determined. Evidence in support of the notion that the maximum radiation harmonic $n_{\max}$ follows the rule, $n_{\max}\omega_0\approx0.5$, has been provided.

---

[1] S. Chu and J. Cooper, Phys. Rev. A **32**, 2769 (1985).

[2] K. Kulander, Phys. Rev. A **35**, 445, (1987).

[3] K. LaGattuta, J. Opt. Soc. Am. B **7**, 639 (1990).

[4] K. Kulander, Phys. Rev. A **38**, 778 (1988).

[5] H. Reiss, Phys. Rev. A **22**, 1786 (1980).

[6] L. Keldysh, Sov. Phys. JETP **20**, 1307 (1965).

[7] K. LaGattuta, Phys. Rev. A **40**, 683 (1989).

[8] G. Kyrala, J. Opt. Soc. Am. B (to be published).

[9] H. Bethe and E. Salpeter, in *Quantum Mechanics of One and Two Electron Atoms* (Springer-Verlag, Berlin 1957).

[10] D. Feng (private communication).

[11] P. Agostini, F. Fabre, G. Maimfray, G. Petite, and N. Rahman, Phys. Rev. Lett. **42**, 1127 (1979).

[12] R. Freeman, T. McIlrath, P. Bucksbaum, and M. Bashkansky, Phys. Rev. Lett. **57**, 3156 (1986).

[13] H. Humpert, H. Schwier, R. Hippler, and H. Lutz, Phys. Rev. A **32**, 3787 (1985).

[14] J. Eberly, Q. Su, and J. Javanainen, J. Opt. Soc. Am. B **6**, 1289 (1989).

[15] L. Brewe, F. Buchinger, M. Ligare, and D. Kelleher, Phys. Rev. A **39**, 3912 (1989); G. Petite, F. Fabre, P. Agostini, M. Crance, and M. Aymar, *ibid.* **29**, 2677 (1984)..